Polyhedron 27 (2008) 3529–3536

Contents lists available at ScienceDirect

Polyhedron

journal homepage: www.elsevier.com/locate/poly

Crystal structures, bioactivities and fluorescent properties of four diverse complexes with a new symmetric benzimidazolic ligand

Chun-Yan Guo [a], Yao-Yu Wang [a,*], Kang-Zhen Xu [b], Hong-Li Zhu [c], Ping Liu [a], Qi-Zhen Shi [a], Shie-Ming Peng [d]

[a] Key Laboratory of Synthetic and Natural Functional Molecule Chemistry of the Ministry of Education, Shaanxi Key Laboratory of Physico-Inorganic Chemistry, Department of Chemistry, Northwest University, Xi'an 710069, China
[b] Department of Chemical Engineering, Northwest University, Xi'an 710069, China
[c] College of Life Sciences, Northwest University, Xi'an 710069, China
[d] Department of Chemistry, National Taiwan University, Taipei, Taiwan

ARTICLE INFO

Article history:
Received 7 July 2008
Accepted 8 August 2008
Available online 4 October 2008

Keywords:
Crystal structure
Water cluster
Biological activity
Fluorescent properties

ABSTRACT

A new ligand, pyridine-3,5-bis(benzimidazole-2-yl) (pbb), and four complexes containing pbb, namely $[pbb(Hpbb)_2]SO_4 \cdot 7H_2O$ (**1**), $[Zn(pbb)_2(H_2O)_4](NO_3)_2 \cdot 2C_2H_5OH \cdot 4H_2O$ (**2**), $[Cd(pbb)_2(H_2O)_4](NO_3)_2 \cdot 2C_2H_5OH \cdot 4H_2O$ (**3**) and $[Zn_2(pbb)_2(\mu\text{-}OH)(\mu\text{-}OAc)](OAc)_2 \cdot 7H_2O$ (**4**) (HOAc = acetic acid), have been designed, synthesized and characterized. Complexes **1–4** show 3D supramolecular architectures that are connected through hydrogen bonds and aromatic π–π interactions. A self-assembled $(H_2O)_{12}$ cluster with a chair conformation $(H_2O)_6$ ring core is observed in **1**, which exhibits an unusual association mode of water molecules. Compounds **2** and **3** present 3D supramolecular structures involving 1D open channels encapsulating NO_3^- ions, and crown-like rings are found in **4**. In addition, the preliminary antibacterial activity of pbb and its complexes were investigated by two methods, which indicate a selective inhibition property for the tested strains. Strong emissions from the complexes were also changed by the coordination modes in the sold state.

1. Introduction

The crystal engineering of supramolecular frameworks based on organic building blocks has made considerable progress in recent years owing to their attractive structural features [1] and potential applications as functional materials in various fields, such as gas storage, electrical conductivity, sensor technology, separation processes, ion exchange, luminescence, magnetism, and catalysis [2–5]. In many cases successful strategies for engineering the assemblies of materials take advantage of non-bonded interactions such as hydrogen-bonding or/and π–π stacking interactions between building blocks. It is well known that organic ligands take crucial roles in the design and construction of desirable supramolecular architectures. Fortunately, benzimidazolic ligands have been proven to be good candidates in respect that the benzimidazolic moieties may be important for providing potential supramolecular recognition sites for π–π aromatic stacking and hydrogen-bonding supramolecular interactions. On the other hand, since Roderick [6] and his co-workers firstly reported that bisbenzimidazoles were potent inhibitors of rhinoviruses in 1972, the study of the bisbenzimidazolyl complexes has increasingly caught researchers' eyes [7]. Attributed to their special physiological activities, some bisbenzimidazolyl complexes have been investigated and even applied in medicine to prevent or cure some diseases [8].

With this background in mind, our attention has been paid to the design and synthesis of a new bisbenzimidazolyl ligand and tuning the self-assembly with metal centers, and further testing their bioactivity. Pyridine-3,5-bis(benzimidazole-2-yl) (pbb; Scheme 1), as a new member for crystal engineering, possesses of a good symmetry and would form versatile coordination modes in the presence of five potential coordination sites. The rich conjugated π backbone of pbb is important to biological systems [9] and also may be applied in the aspects of potential fluorescent materials for electroluminescence and optical switching devices [10]. According to all the above, we have much interest in the design and syntheses of pbb and its complexes. Herein, we report the syntheses and structural characterization of pbb, $[pbb(Hpbb)_2]SO_4 \cdot 7H_2O$ (**1**), $[Zn(pbb)_2(H_2O)_4](NO_3)_2 \cdot 2C_2H_5OH \cdot 4H_2O$ (**2**), $[Cd(pbb)_2(H_2O)_4](NO_3)_2 \cdot 2C_2H_5OH \cdot 4H_2O$ (**3**) and $[Zn_2(pbb)_2(\mu\text{-}OH)(\mu\text{-}OAc)](OAc)_2 \cdot 7H_2O$ (**4**), whose fluorescent properties and preliminary biological tests have been explored.

* Corresponding author. Tel./fax: +86 029 88303798.
E-mail address: wyaoyu@nwu.edu.cn (Y.-Y. Wang).

0277-5387/$ - see front matter © 2008 Elsevier Ltd. All rights reserved.
doi:10.1016/j.poly.2008.08.018

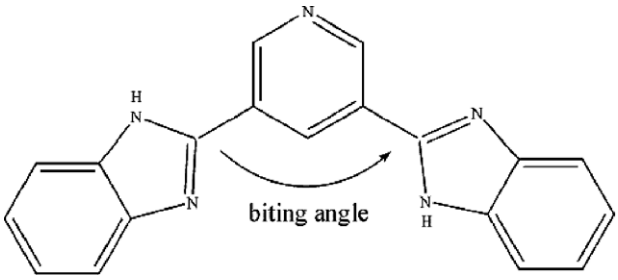

Scheme 1. Schematic view of pyridine-3,5-bis(benzimidazole-2-yl).

2. Experimental

2.1. Materials and analyses

All reagents and solvents were used directly as supplied commercially without further purification, except that the ligand (pbb) was prepared. Elemental analyses (C, H, and N) were determined with a Perkin–Elmer model 240 °C automatic instrument. Infrared spectra on KBr pellets were performed in a BRUKER EQUINOX–55 spectrometer in the range of 4000–400 cm^{-1}. ^1H NMR spectra were recorded using an INOVA–400 MHZ (Varian, America). Mass spectra were obtained with a JEOL HX–110 HF double focusing spectrometer operating in the positive ion detection mode. A Micro DSC III Thermal Activity Monitor (Setaram, France) was used to determine the power-time curves of *Escherichia coli* growth.

2.2. Syntheses

The formation of **1**, **2**, **3,** and **4** with the experimental conditions are shown in Scheme 2. Their syntheses are given in the sequel.

2.2.1. Preparation of the ligand

The ligand (pbb) was prepared from o-phenylenediamine and 3,5-pyridinedicarboxylic acid monohydrate by a modified literature method [11]. The product was a pale-yellow powder in 60% yield, mp > 280 °C. *Anal.* Calc. for $C_{19}H_{13}N_5$: C, 73.29; H, 4.21; N, 22.49. Found: C, 73.28; H, 4.18; N, 22.50%. IR (cm^{-1}, KBr): 3386 (s), 3185 (s), 2930 (s), 1602 (w), 1514 (w), 1437 (m), 1322 (w), 1279 (m), 1224 (w), 1118 (w), 1016 (w), 959 (w), 898 (w), 734 (s), 699 (m). MS (FAB): *m/z* (%) = 312.3 (pbb). ^1H NMR (ppm, DMSO): δ = 9.319 (s, 1H, 1-H), 9.426 (s,2H,2-H), 13.347 (s, 2H, 3-H), 7.682 (dd, 4H, 4-H), 7.281 (m, 4H, 5-H).

2.2.2. $[pbb(Hpbb)_2]SO_4 \cdot 7H_2O$ (**1**)

A mixture of pbb (31 mg, 0.1 mmol), $ZnSO_4 \cdot 7H_2O$ (29 mg, 0.1 mmol) and 10 mL H_2O was sealed in a 25 mL Telfon-lined stainless steel container, which was heated to 140 °C for 72 h. After cooling to room temperature at a rate of 2 °C per hour, well-shaped yellow block crystals of **1**, suitable for X-ray diffraction, were obtained. The final pH value of the mixture was about 5. Notably, **1** was obtained under the emergence of $ZnSO_4$. It has been confirmed that the existence of $ZnSO_4$ is required in this process, although the mechanism is not clear. *Anal.* Calc. for $C_{57}H_{57}N_{15}O_{12}S$ (1176.24): C, 58.20; H, 4.88; N, 17.86. Found: C, 58.20; H, 4.89; N, 17.88%. IR (cm^{-1}, KBr): 3745 (m), 3381 (s), 1596 (m), 1490 (w), 1429 (s), 1342 (m), 1312 (m), 1275 (m), 1254 (m), 1137 (w), 1015 (w), 955 (w), 896 (w), 857 (w), 742 (s), 616 (m).

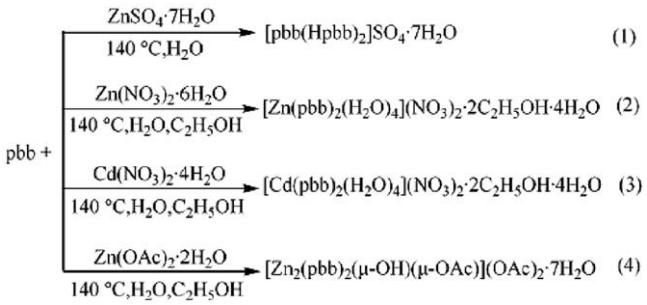

Scheme 2. The formation of **1**–**4** together with the experimental conditions.

2.2.3. $[Zn(pbb)_2(H_2O)_4](NO_3)_2 \cdot 2C_2H_5OH \cdot 4H_2O$ (**2**)

A mixture of pbb (31 mg, 0.1 mmol), $Zn(NO_3)_2 \cdot 6H_2O$ (30 mg, 0.1 mmol) and 10 mL water–ethanol (1:1) was sealed in a 25 mL Telfon-lined stainless steel container, which was heated to 140 °C for 72 h. Slow cooling of the reaction mixture to room temperature gave light-yellow block crystals in ca. 60% yield. *Anal.* Calc. for $C_{42}H_{54}N_{12}O_{16}Zn$ (1048.34): C, 48.12; H, 5.19; N, 16.03. Found: C, 48.11; H, 5.14; N, 16.02%. IR (cm^{-1}, KBr): 3443 (s), 1764 (w), 1628 (m), 1481 (m), 1385 (s), 1224 (m), 1025 (w), 904 (w), 826 (w), 743 (m), 693 (w).

2.2.4. $[Cd(pbb)_2(H_2O)_4](NO_3)_2 \cdot 2C_2H_5OH \cdot 4H_2O$ (**3**)

The preparation of **3** was similar to that of **2** except that $Cd(NO_3)_2 \cdot 4H_2O$ (0.1 mmol) was used instead of $Zn(NO_3)_2 \cdot 6H_2O$. Pale-yellow block crystals were obtained in ca. 66% yield. *Anal.* Calc. for $C_{42}H_{54}N_{12}O_{16}Cd$ (1095.37): C, 46.05; H, 4.97; N, 15.34. Found: C, 46.04; H, 4.96; N, 15.36%. IR (cm^{-1}, KBr): 3467 (s), 1763 (w), 1623 (m), 1478 (m), 1423 (m), 1383 (s), 1225 (w), 1123 (w), 1045 (w), 961 (w), 901 (w), 826 (w), 735 (m), 690 (m).

2.2.5. $[Zn_2(pbb)_2(\mu\text{-}OH)(\mu\text{-}OAc)](OAc)_2 \cdot 7H_2O$ (**4**)

The preparation of **4** was similar to that of **2** except that $Zn(OAc)_2 \cdot 2H_2O$ (0.1 mmol) was used instead of $Zn(NO_3)_2 \cdot 6H_2O$. Pale-yellow block crystals were obtained in ca. 48% yield. *Anal.* Calc. for $C_{44}H_{50}N_{10}O_{14}Zn_2$ (1073.68): C, 49.22; H, 4.69; N, 13.04. Found: C, 49.24; H, 4.69; N, 13.10%. IR (cm^{-1}, KBr): 3121 (s), 1591 (s), 1482 (m), 1430 (m), 1332 (m), 1277 (m), 1227 (w), 1184 (w), 1132 (w), 1051 (w), 1021 (w), 960 (w), 932 (w), 903 (w), 847 (w), 744 (s), 699 (s), 614 (w).

2.3. X-ray crystallography

Diffraction experiments for **1**, **2**, **3,** and **4** were carried out with Mo Kα radiation using a BRUKER SMART APEX CCD diffractometer at 293 (2) or 296 (2) K. The structures were solved by direct methods and refined with the full-matrix least-squares technique on F^2 using the SHELXS–97 and SHELXL–97 [12] programs. All non-hydrogen atoms were refined anisotropically. A summary of the crystallographic data and structure refinement is shown in Table 1, selected bond lengths and angles of the complexes are listed in Table 2, and possible hydrogen bond geometries are given in Table 3.

2.4. Biological activity tests

Bacteria (*E. coli*, *Staphylococcus aureus,* and *Bacillus subtilis)* and mould (*Glomerella cingulata*, *Alternaria solani,* and *Monilinia fructicola)* strains were provided by the College of Life Sciences at Northwest University (China). The antimicrobial activities of pbb and its complexes were examined by the bacteriostatic ring test method. The antibacterial activity was measured as the diameter of the inhibitory zones in the soft agar layer stained after 24 h incubation at 37 °C, while inhibition again mould after 72 h at 28 °C. An inhibitory zone with a diameter less than 6 mm corresponds to lack of activity (6 mm is the diameter of the spot). Control experiments with solvents show that the solvents have no activity. Selected duplicates were run to ensure reproducibility.

Table 1
Crystal data and structure refinements for complexes **1**–**4**

Complexes	**1**	**2**	**3**	**4**
Empirical formula	$C_{57}H_{57}N_{15}O_{12}S$	$C_{42}H_{54}N_{12}O_{16}Zn$	$C_{42}H_{54}N_{12}O_{16}Cd$	$C_{44}H_{50}N_{10}O_{14}Zn_2$
Formula mass	1176.24	1048.34	1095.37	1073.68
Temperature (K)	293(2)	296(2)	296(2)	296(2)
Crystal system	triclinic	triclinic	triclinic	monoclinic
Space group	$P\bar{1}$	$P\bar{1}$	$P\bar{1}$	$C2/c$
a (Å)	12.495(3)	7.690(3)	7.888(2)	16.7513(14)
b (Å)	15.367(3)	11.015(4)	11.214(3)	13.5444(12)
c (Å)	15.976(3)	15.332(6)	15.004(4)	20.7377(19)
α (°)	73.050(3)	70.791(7)	70.349(5)	90
β (°)	72.760(3)	89.738(7)	88.439(5)	95.5710(10)
γ (°)	82.380(3)	75.442(7)	74.617(5)	90
V (Å^3)	2798.9(10)	1182.87(7)	1202.3(5)	4682.9(7)
Z	2	1	1	4
D_{calc} (g cm^{-3})	1.396	1.472	1.513	1.523
μ (mm^{-1})	0.136	0.603	0.537	1.103
F[000]	1232	548	566	2224
θ (°)	2.47–25.50	1.41–25.10	2.00–25.09	1.94–25.10
Data/restraints/parameters	10346/0/766	4136/0/356	4175/12/356	4166/0/319
Goodness-of-fit on F^2	0.992	0.861	0.870	1.058
Final R[a] indices [$I > 2\sigma(I)$]	$R_1 = 0.0735$	$R_1 = 0.0666$	$R_1 = 0.0566$	$R_1 = 0.0495$
	$wR_2 = 0.1680$	$wR_2 = 0.1494$	$wR_2 = 0.1332$	$wR_2 = 0.1139$
R indices (all data)	$R_1 = 0.1524$	$R_1 = 0.1547$	$R_1 = 0.1021$	$R_1 = 0.0875$
	$wR_2 = 0.2134$	$wR_2 = 0.1814$	$wR_2 = 0.1590$	$wR_2 = 0.1349$

[a] $R_1 = \sum(|F_0| - |F_C|)/\sum|F_0|$; $wR_2 = [\sum w(|F_0^2| - |F_C^2|)^2/\sum w(|F_0^2|)^2]^{1/2}$.

Table 2
Selected bond lengths (Å) and angles (°) for complexes **1**–**4**

Complex **1**			
N(1)–C(7)	1.327(5)	N(2)–C(7)	1.349(5)
N(4)–C(13)	1.334(5)	N(5)–C(13)	1.361(5)
N(6)–C(26)	1.368(5)	N(7)–C(26)	1.306(5)
N(9)–C(32)	1.331(5)	N(10)–C(32)	1.353(5)
N(11)–C(45)	1.359(5)	N(12)–C(45)	1.323(5)
N(14)–C(51)	1.349(5)	N(15)–C(51)	1.346(5)
N(1)–C(7)–C(8)	126.9(3)	N(5)–C(13)–C(11)	125.3(3)
N(6)–C(26)–C(27)	124.5(4)	N(9)–C(32)–C(29)	125.7(4)
N(11)–C(45)–C(46)	124.0(3)	N(14)–C(51)–C(49)	125.2(3)
Complex **2**			
Zn(1)–O(1)	2.112(5)	Zn(1)–O(2)	2.098(4)
Zn(1)–N(1)	2.158(5)	O(2)–Zn(1)–O(1)	86.8(2)
O(1)–Zn(1)–N(1)	89.5(2)	O(2)–Zn(1)–N(1)	86.9(2)
Complex **3**			
Cd(1)–O(1)	2.30(1)	Cd(1)–O(2)	2.30(1)
Cd(1)–N(3)	2.32(1)	O(2)–Cd(1)–O(1)	84.0(5)
O(2)–Cd(1)–N(3)	94.2(5)	O(1)–Cd(1)–N(3)	90.8(4)
Complex **4**			
Zn(1)–O(1)	1.970(3)	Zn(1)–O(2)	1.916(2)
Zn(1)–O(3)	1.956(3)	Zn(1)–N(1)	2.063(3)
O(2)–Zn(1)–O(3)	127.7(2)	O(2)–Zn(1)–O(1)	108.3(2)
O(3)–Zn(1)–O(1)	110.7(2)	O(2)–Zn(1)–N(1)	101.8(1)
O(3)–Zn(1)–N(1)	100.1(2)	O(1)–Zn(1)–N(1)	105.0(2)

Microcalorimetry is an important tool for measuring metabolic activities of cells and biological tissues [13]. Here, the power-time curves for growth of *E.* coli at 37 °C were determined in the presence of pbb and its complexes by using a microcalorimetric method. In the exponential growth phase of *E. coli*, the thermal power given out by the microbe and time are related with the following equation [14]:

$$\ln P_t = \ln P_o + kt$$

where P_t and P_0 are the thermal power at time t and t_0, respectively, k is the growth rate constant. Using the experimental data, P_t and t obtained from the thermal power-time curves under various concentrations of the samples, the corresponding growth rate constant k can be calculated from linear regression analysis. Under the same cultivation conditions, the experimental results (the thermal power-time curves) display high repeats.

Table 3
Hydrogen-bonding geometries for complexes **1**–**4**

D–H···A	D–H (Å)	H···A (Å)	D···A (Å)	D–H···A (°)
Complex **1**				
O(1)–H(1W)···O(3)	0.84	1.92	2.762(6)	177.5
O(3)–H(6W)···O(2)	0.85	2.23	3.079(7)	179.4
O(4)–H(7W)···O(3)	0.83	1.84	2.594(6)	150.5
O(5)–H(9W)···O(4)	0.85	2.44	2.899(7)	114.4
O(5)–H(10W)···O(12)#2	0.85	1.83	2.651(4)	161.7
O(6)–H(11W)···O(9)	0.85	2.02	2.866(5)	179.3
O(8)–H(15W)···O(4)#2	0.83	1.97	2.747(5)	154.0
N(9)–H(9D)···O(6)	0.86	1.79	2.625(5)	162.2
N(5)–H(5D)···O(12)#2	0.86	1.92	2.759(4)	165.9
N(1)–H(1D)···O(5)	0.86	1.80	2.625(4)	159.2
N(14)–H(14D)···O(11)	0.86	1.91	2.728(4)	157.3
Complex **2**				
O(1)–H(1WB)···O(8)#1	0.832	1.871	2.691	167.85
O(2)–H(2WA)···O(7)	0.827	1.905	2.720	168.24
O(2)–H(2WB)···O7#2	0.828	2.054	2.790	147.84
O(7)–H(7WB)···O(8)	0.835	2.044	2.792	148.69
N(2)–H(2A)···O(3)	0.860	2.152	2.999	168.29
Complex **3**				
O(1)–H(1A)···O(8)#1	0.832	1.889	2.681	158.76
O(7)–H(7B)···O(8)#2	0.837	1.963	2.793	170.84
N(4)–H(4A)···O(3)	0.860	1.981	2.825	166.63
N2-H2A···O(5)#3	0.860	2.190	3.039	169.27
Complex **4**				
O(7)–H(7B)···O(3)	0.81	2.06	2.862(4)	169.0
O(7)–H(7C)···O(5)#4	0.82	1.96	2.751(3)	161.6
O(6)–H(6B)···O(7)	0.85	2.03	2.870(5)	169.0
O(6)–H(6C)···O(8)	0.85	1.87	2.689(5)	161.5
O(8)–H(8B)···O(2)#4	0.82	1.99	2.790(5)	164.3

For **1**: #2 $-x+1$, $-y+1$, $-z+1$. For **2**: #1 $-x+1$, $-y+1$, $-z+1$; #2 $-x$, $-y+1$, $-z+1$. For **3**: #1 $x, y, z-1$; #2 $-x+1$, $-y+1$, $-z+1$; #3 $-x+1$, $-y+1$, $-z$. For **4**: #4 $x-1/2$, $y-1/2$, z.

3. Results and discussion

The pale-yellow powder pbb is obtained in good yield. In order to confirm the identity of the product, the MS and ^{1}H NMR spectra of pbb were measured, and the spectra are given in Fig. S1.

3.1. Description of structures

3.1.1. Crystal Structure of **1**

The single-crystal X-ray structural analysis of complex **1** reveals a H_2SO_4 solvate of pbb, in which three pbb molecules, eight water molecules and one SO_4^{2-} ion are observed. As shown in Fig. 1a, two of the three pbb molecules are protonated, and intramolecular dihedral angels between the benzimidazolic rings are 9.04, 12.31, and 3.92 °. The bite angles of the three rings are 125.97, 133.69, and 124.56 °, respectively. The above data suggest that the middle pbb molecule may be potentially affected by the other two via π–π stacking interactions. Notably, there are O–H···O hydrogen bonds and weak O···O interactions in the unit of **1**, forming 1D chains in which three six-membered rings and one four-membered ring units are alternately arranged (Fig. S2).

The most striking feature of these chains is that the six-membered rings formed by free water molecules adopt a chair conformation (Fig. 1b), of which four oxygen atoms are located in the same geometry plane (O···O···O angles: 71.372° and 108.628°) and the remaining two oxygen atoms are symmetrically arranged on the bilateral sides of the plane (the dihedral angel between the plane O1A, O2, O3 and the plane O1A, O2, O1 is 49.39°). Here, the hexameric water cluster is unlike the previously published hexamer clusters [1b,15]. In the inter-$(H_2O)_6$ rings, water–water connections have an average O···O distance of 2.853 Å, which is very close to the corresponding value observed in liquid water (2.85 Å) [16] and longer than corresponding value of 2.759 Å in hexagonal ice (I_h) [17]. The emergence of a chair conformation, to some extent, may have a significant effect on the construction of a stable supramolecular network. Further, each $(H_2O)_6$ subunit and two $(H_2O)_3$ subunits are associated to form a centrosymmetric $(H_2O)_{12}$ cluster by hydrogen-bonds. Two dangling trimeric water molecules at the periphery are situated alternately right and left of the $(H_2O)_6$ subunit, so as to associate with the SO_4^{2-} ion. A closer view of the $(H_2O)_{12}$ cluster illustrates that each water monomer, except for O8, acts as both a hydrogen-bonding donor and acceptor. In the supramolecular $(H_2O)_{12}$ morphology, the O···O distances range from 2.592 to 3.079 Å, resulting in an average O···O distance of 2.800 Å, which is very close to those observed in liquid water (2.80 Å) [18] and comparable to the corresponding value in the ice phase (2.77–2.84 Å) [19]. However, the O···O···O angles vary widely (ca. 71.439–131.023°) with an average of 102.447°, considerably deviating from the preferred ideal tetrahedral geometry of water. Compared with other water morphologies reported recently [20], our observation of $(H_2O)_{12}$ clusters in such a water framework may be due to its different interactions with surrounding water molecules and the SO_4^{2-} ions. The present association mode of the $(H_2O)_{12}$ cluster, comprising of a chair conformation $(H_2O)_6$ ring core and the additional two dangling trimeric water clusters, in **1** is rather unusual.

Moreover, 1D supramolecular chains are linked with pbb molecules through N···O hydrogen-bonding to give rise to 2D layers (Fig. S3). The adjacent layers are connected further to afford a 3D supramolecular structure, in which face-to-face π–π stacking interactions between the aromatic rings (centroid-to-centroid distances: 3.531, 3.598, 3.616, and 3.658 Å) are dominant.

3.1.2. Crystal structures of ***2*** and ***3***

Complexes **2** and **3** are isomorphous, and thus only the structure of **2** is described here in detail. Complex **2** crystallizes in the triclinic space group $P\bar{1}$ and is composed of a mononuclear unit. The coordination geometry around each Zn^{II} atom can be attributed to a slightly distorted octahedron with four water molecules in the equatorial sites and two nitrogen atoms from pyridine rings of two pbb molecules in the axial positions (Fig. 2a). The Zn–N (2.158 Å) and Zn–O (2.112 and 2.098 Å) bond lengths are in the normal range and are similar to those of mononuclear Zn^{II} complexes reported in literature [21]. The biting angle of pbb in **2** is 123.27°, and the intramolecular dihedral angel between the benzimidazole groups is 4.87°, which are different from the corresponding values in **1**. As expected, hydrogen-bonding and π–π stacking interactions are also present, arranging and stabilizing of the

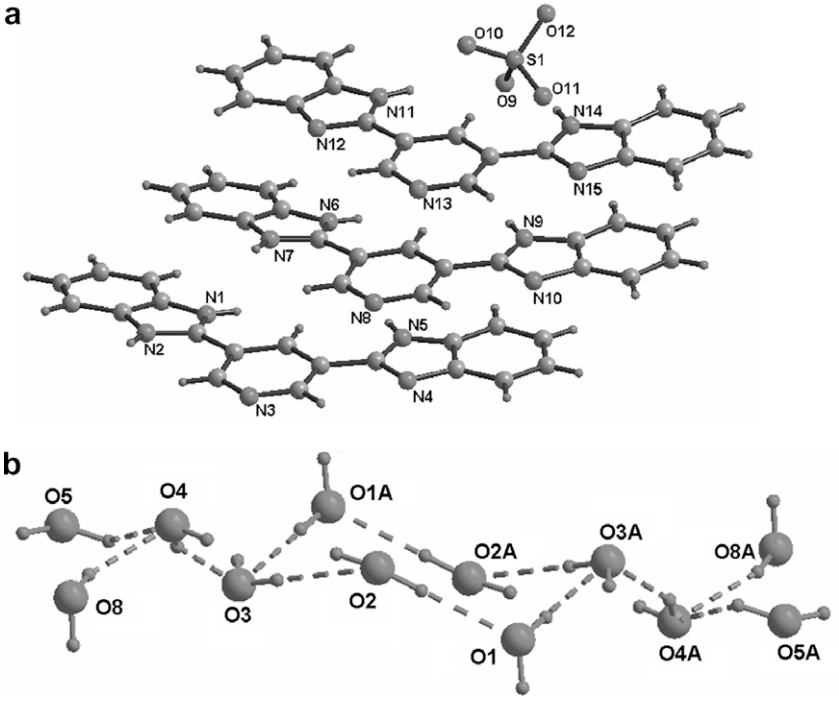

Fig. 1. (a) Molecular structure of **1** (the water molecule is omitted for clarity); (b) Perspective view of the discrete $(H_2O)_{12}$ cluster containing a chair conformation. Dash lines show the hydrogen bonding between water molecules.

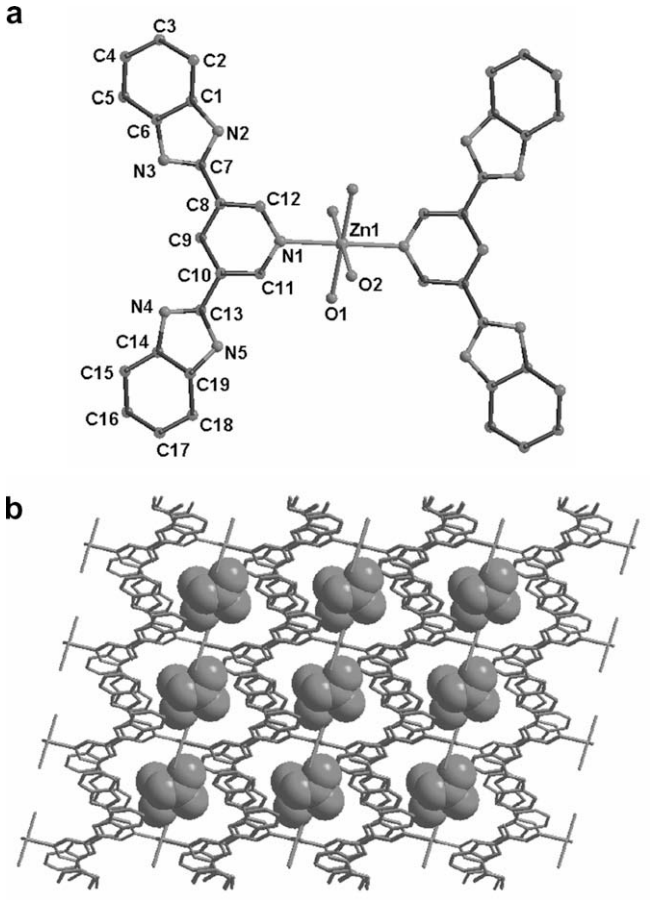

Fig. 2. (a) View of the coordination environment of Zn(II) in **2**; (b) 3D network of **2** containing 1D open channels encapsulating NO_3^- ions.

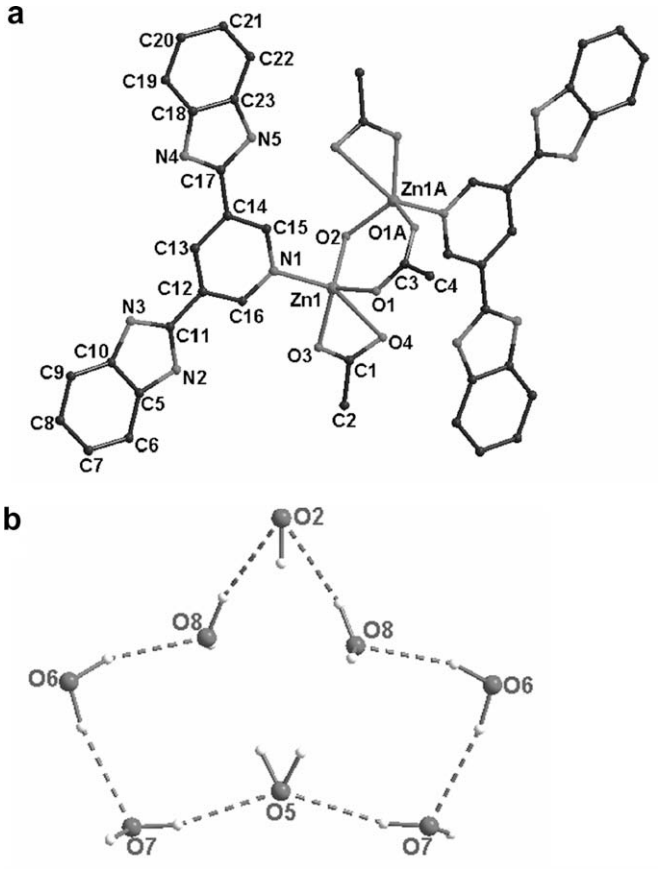

Fig. 3. (a) Coordination environment of Zn(II) in **4**; (b) Perspective view of the crown-like ring formed by hydrogen bonding.

supramolecular framework of **2**. There exist intense O–H···O interactions between the coordinated water and the free water, forming 1D chair chains (Fig. S4). The range of the O···O distances is approximately from 2.690 to 2.791 Å. It is interesting that four oxygen atoms (O2, O2A, O7, and O7A) are arranged in one plane, whilst O8 and O8A are symmetrically arranged on both sides of the plane. That is, similar to **1**, a chair conformation is built by these six oxygen atoms in **2**. The dihedral angel between the plane O1A, O2, O3 and the plane O1A, O2, O1 is 52.43°. Further, the 1D chair chains are connected into a 2D layered structure via weak N···O interactions (2.748 and 2.786 Å) and strong π–π stacking interactions between the two imidazole rings (minimum centroid-to-centroid distance: 3.512 Å) (Fig. S5). Adjacent 2D layers are further linked by hydrogen bonds (N2–H2···O3 2.999 Å) to give a 3D structure with 1D open channels encapsulating NO_3^- ions (Fig. 2b).

3.1.3. Crystal structure of *4*

Unlike **2** and **3**, the basic structure of **4** consists of a binuclear unit (Fig. 3a). The Zn^{II} center in **4** is four-coordinate with a distorted tetrahedral geometry, and is coordinated by one nitrogen atom in the pyridine ring of pbb and one oxygen atom in an acetate group. Zn1 and Zn1A are linked by one μ_2-OH (O2) and one μ_2-OAc (O1, O1A) with a Zn1···Zn1A distance of 3.215 Å. The bite angle of pbb in **4** is 123.55° and this is similar to that found in **2**. However, the intramolecular dihedral angels between the benzimidazole groups in **4** are 2.60°, which is very different to those of **1** and **2**. The bond distances of Zn–N and Zn–O in **4** are shorter than those in **2**, which may be as a result of the different coordination environment of Zn^{II}. Similar to **2**, there also exist rich hydrogen-bonding and strong π–π stacking interactions in **4**. A 1D chain (Fig. S6) is obtained due to hydrogen bonding interactions (O7–H7···O3 2.862, O7–H7···O5 2.751 Å) between three lattice water molecules and the oxygen atoms of the acetate groups. Interestingly, free water and the bridge oxygen (O2) are associated by hydrogen bonding to form a crown-like ring, as shown in Fig. 3b. In the eight-membered ring, the O···O distances fall in the range 2.696–2.868 Å, with an average of 2.768 Å, which is very close to the corresponding value of 2.759 Å in ice I_h [17], but is shorter than those observed in containing-water rings [16a,22]. This might be attributed to its different modes of connectivity with the surrounding water molecules. Furthermore, these rings link adjacent 1D chains to give rise to a 2D layered supramolecular structure (Fig. S7). Strong face-to-face π–π stacking interactions (minimum centroid-to-centroid distance 3.517 Å) contribute to the stabilization of the 3D supramolecular network of **4**. Additional hydrogen bonds involve the coordinated/uncoordinated carboxylate oxygen atoms, uncoordinated nitrogen atoms and free water molecules.

3.2. Biological results and discussion

3.2.1. Inhibitory zone test method

The antimicrobial activities of pbb and its complexes (**2**, **3**, and **4**) against bacteria (*E. coli*, *S. aureus*, and *B. subtilis*) and mould (*G. cingulata*, *M. fructicola*, *A. solani*) were examined by the inhibitory zone test method. The selected results obtained by this method are shown in Fig. 4. In this model, it could turn out that the samples have some antibacterial activity against the selected strains, the diameter of the inhibitory zone ranges from 7 to 25 mm. Inhibition

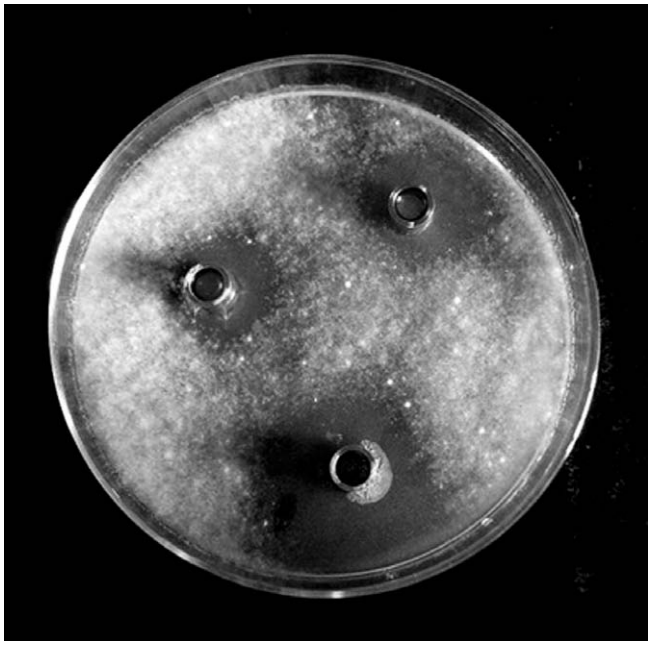

Fig. 4. Effect of concentrations of **2** on the growth of *Alternaria solani*: top left—2.5 μg mL^{-1}; top right—5 μg mL^{-1}; bottom—7.5 μg mL^{-1}.

again mould was observed clearly, whilst when the moulds were replaced by bacteria, there was a general decrease in activity. The ability of the samples to inhibit growth of the tested strains is listed in Table 4. From the viewpoint of the test, four samples exhibit only poor activity against *E. coli* and *S. aureus*, but an inhibition ring with a diameter of 7–8 mm against *B. subtilis* was found. Comparatively, it seems that the germproof ability of the samples against mould is superior to that against bacteria. However, different strains result in a different antibacterial effect of the samples. The average inhibitive ring diameters are, respectively, 21 mm (*G. cingulata*), 13 mm (*M. fructicola*) and 24 mm (*A. solani*). In addition, the antibacterial activity of pbb and its complexes against the same strain give distinctness. The ligand pbb presents optimal antibacterial activity versus *G. cingulata* and *A. solani* whereas **2–4** have good antibacterial activity against *M.* fructicola and are slightly active against *B. subtilis*.

These results indicate that pbb and its complexes possess selective antimicrobial properties for the tested objects. That is, they maybe possess higher antimicrobial activities against mould than bacteria. Consequently, pbb and its complexes are expected to have higher special bio-activity through further survey.

3.2.2. Microcalorimetric method

On the other hand, the antimicrobial activities of pbb and **2–4** were also investigated by the microcalorimetric method. Take *E. coli* as an example. Their partly thermal power-time (p–t) curves at 37 °C are shown in Fig. 5. All the curves are similar in shape,

Table 4
Biological results[a]

Sample	pbb	2	3	4
Escherichia coli	–	–	–	–
Bacillus subtilis	+	+	+	+
Staphylococcus aureus	–	–	–	–
Glomerella Cingulata	++	+	+	+
Alternaria Solani	++	+	+	+
Monilinia fructicola	+	++	++	++

[a] –, weak or no inhibition; +, inhibition; ++, strong inhibition.

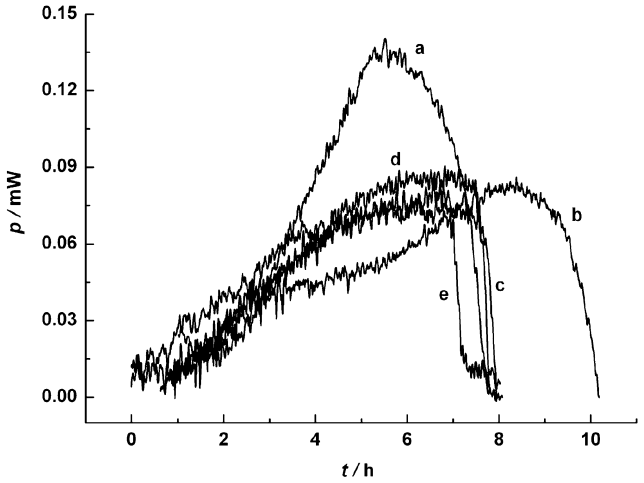

Fig. 5. Power–time curves of *E. coli* at 37 °C under different conditions in: (a) blank; (b) pbb, c = 2 μg mL^{-1}; (c) **2**, c = 2 μg mL^{-1}; (d) **3**, c = 5 μg mL^{-1}; (e) **4**, c = 3 μg mL^{-1}.

which testifies the good reappearance using this method. However, the thermal powers in the growth phase for *E. coli* are reduced evidently in the presence of pbb or its complexes. This result shows that the samples (pbb, **2**, **3**, and **4**) can inhibit the growth of *E. coli*.

According to the p–t curves, the corresponding growth rate constant k can be calculated from linear regression analysis. The k versus c curves of pbb and **2–4** were obtained, as illustrated in Fig. 6. The k value is ca. 0.83 h^{-1} when the concentration of the samples is 0 μg mL^{-1}. It can be seen that the k values clearly decrease due to the addition of the samples. The results can be described that pbb and its complexes exhibit good activities against *E. coli*. In the concentration range 2–100 μg mL^{-1}, the k values increase, then decrease. Therefore it may be predicted that the concentration of the samples is important to the antibacterial action [23]. What is more, one concentration peak value c_p can be observed in every k–c curve. It is clear that the c_p values of **2–4** are less than that of pbb. It could be deduced that, under the same conditions, the antibacterial actions of the complexes against *E. coli* are superior to that of the ligand. That means the presence of metal ions has improved the antibacterial activity of ligand. Accordingly, we believe that this work may contribute basic information to the further

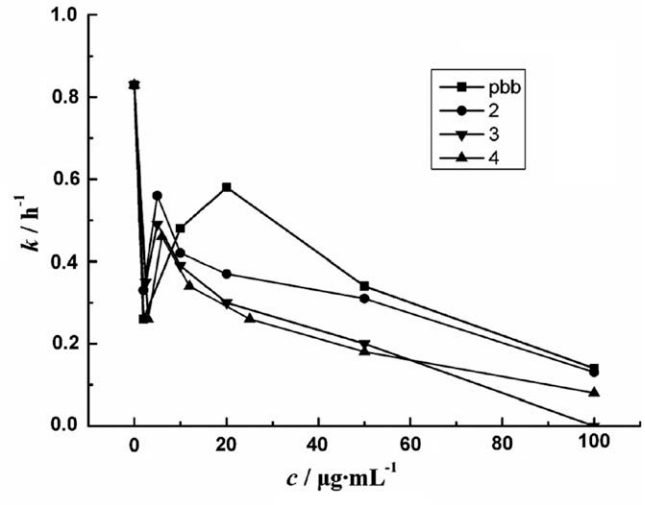

Fig. 6. The k–c curves of *E. coli* at 37 °C with different concentrations of pbb, **2**, **3**, and **4**.

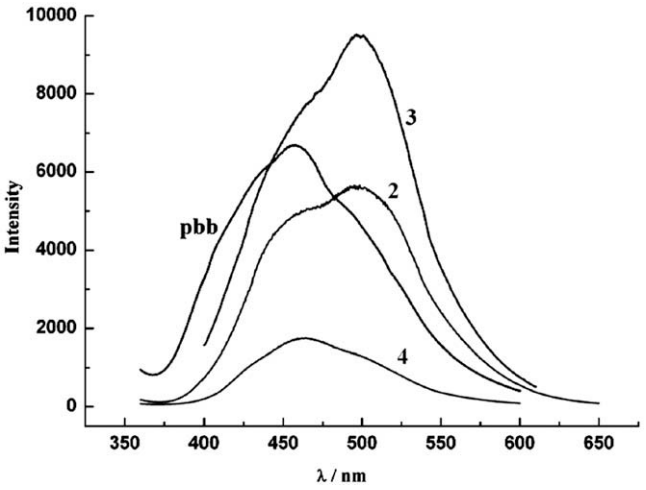

Fig. 7. Solid-state fluorescence emission spectra of pbb, **2**, **3**, and **4** at room temperature.

application of pbb and its complexes in the field of biological chemistry.

3.3. Fluorescent properties

The solid-state fluorescent properties of pbb and complexes **2–4** were investigated at room temperature (Fig. 7). Free pbb exhibits an intense emission peak at 458 nm upon excitation at 320 nm. The emission should be assigned to the intraligand π–π^* transitions. Excitation at 300 nm leads to a fluorescent emission band at about 465 nm for **4**. The emission spectra of **2** and **3** show a main peak at 498 nm (λ_{ex} = 305 nm) and 497 nm (λ_{ex} = 340 nm), respectively. It can be seen that complexes **2–4** clearly exhibit a red-shift with respect to free pbb. We tentatively assign it to a ligand-to-metal charge transfer (LMCT) [1g]. The differences of the peak positions may be considered to be a result of the dissimilar coordination of the metal centers because the emission behavior is closely associated to the metal ions and ligands around them [1d]. These complexes may be good candidates for stable fluorescent materials.

4. Conclusion and perspectives

In this paper, we have successfully synthesized a new ligand, pbb, and four of its complexes with different architectures and properties. It is worth mentioning that a rarely known discrete $(H_2O)_{12}$ cluster, with a chair conformation, and a crown-like eight-membered ring have been observed in **1**–**4**. These results indicate that these complexes enrich the supramolecular chemistry of organic aromatic derivatives. Our studies also show that hydrogen-bonding, π–π stacking interactions and weak interaction between atoms play a crucial role in connecting the low-dimensional units into high-dimensional supramolecular structures. Importantly, the strong fluorescent properties and the selective bioactivity of pbb and **2**–**4** make them excellent candidates for potential photoactive materials and bio-inhibitors. Further studies will focus on the construction of new metal-organic coordination polymers from pbb, and their bioactivities.

Acknowledgement

This work was supported by the National Natural Science Foundation of China (Grant No. 20771090), TRAPOYT and the Specialized Research Fund for the Doctoral Program of Higher Education (No. 20050697005).

Appendix A. Supplementary data

CCDC 690764, 690765, 691177 and 690766 contain the supplementary crystallographic data for **1**, **2**, **3,** and **4**. These data can be obtained free of charge via http://www.ccdc.cam.ac.uk/conts/retrieving.html, or from the Cambridge Crystallographic Data Centre, 12 Union Road, Cambridge CB2 1EZ, UK; fax: (+44) 1223-336-033; or e-mail: deposit@ccdc.cam.ac.uk. Supplementary data associated with this article can be found, in the online version, at doi:10.1016/j.poly.2008.08.018.

References

[1] (a) R.L. Sang, L. Xu, Inorg. Chem. 44 (2005) 3731;
(b) Y.P. Wu, C.J. Wang, Y.Y. Wang, P. Liu, W.P. Wu, Q.Z. Shi, S.M. Peng, Polyhedron 25 (2006) 3533;
(c) K.T. Holman, A.M. Pivovar, J.A. Swift, M.D. Ward, Acc. Chem. Res. 34 (2001) 107;
(d) X.L. Wang, Y.F. Bi, G.C. Liu, H.Y. Lin, T.L. Hu, X.H. Bu, CrystEngCommun 10 (2008) 349;
(e) Y.T. Wang, G.M. Tang, W.Y. Ma, W.Z. Wan, Polyhedron 26 (2007) 782;
(f) M. Du, Z.H. Zhang, X.J. Zhao, H. Cai, Cryst. Growth Des. 6 (2006) 114;
(g) G.B. Che, C.B. Liu, B. Liu, Q.W. Wang, Z.L. Xu, CrysEngCommun 10 (2008) 84;
(h) X.P. Zhou, W.X. Ni, S.Z. Zhan, J. Ni, D. Li, Y.G. Yin, Inorg. Chem. 46 (2007) 2345.
[2] (a) M.P. Hogerheide, J. Boersma, G.V. Koten, Coord. Chem. Rev. 155 (1996) 87;
(b) D. Imbert, M. Cantuel, J.-C.G. Bünzli, G. Bemardinelli, C. Piguet, J. Am. Chem. Soc. 125 (2003) 15698;
(c) N.M. Shavaleev, L.P. Moorcraft, S.J.A. Pope, Z.R. Bell, S. Faulkner, M.D. Ward, Chem. Commun. (2003) 1134;
(d) S.I. Klink, H. Keizer, F.C.J.M. van Veggel, Angew. Chem., Int. Ed. 39 (2000) 4319.
[3] (a) M. Albrecht, M. Lutz, A.L. Spek, G. van Koten, Nature 406 (2000) 970;
(b) C.D. Wu, A. Hu, L. Zhang, W. Lin, J. Am. Chem. Soc. 127 (2005) 8940;
(c) D.N. Dybtsev, H. Chun, S.H. Yoon, D. Kim, K. Kim, J. Am. Chem. Soc. 126 (2004) 1308;
(d) K. Uemura, S. Kitagawa, M. Knodo, K. Fukui, R. Kitaura, H.C. Chang, T. Mizutani, Chem. Eur. J. 8 (2002) 3587;
(e) M.H. Zeng, X.L. Feng, X.M. Chen, J. Chem. Soc., Dalton Trans. (2004) 2217;
(f) O.M. Yaghi, H. Li, J. Am. Chem. Soc. 118 (1996) 295.
[4] (a) B.J. Holliday, C.A. Mirkin, Angew. Chem., Int. Ed. 40 (2001) 2022;
(b) J.W. Steed, J.L. Atwood, Supramolecular Chemistry, Wiley, Chichester, UK, 2000.
[5] (a) B. Zhao, H.L. Gao, X.Y. Chen, P. Cheng, W. Shi, D.Z. Liao, S.P. Yan, Z.H. Jiang, Chem. Eur. J. 12 (2006) 149;
(b) C.S. Liu, X.S. Shi, J.R. Li, J.J. Wang, X.H. Bu, Cryst. Growth Des. 6 (2006) 656;
(c) Q. Yue, J. Yang, G.H. Li, G.D. Li, W. Xu, J.S. Chen, S.N. Wang, Inorg. Chem. 44 (2005) 5241;
(d) B.Q. Ma, D.S. Zhang, S. Gao, T.Z. Jin, C.H. Yan, Angew. Chem., Int. Ed. 39 (2000) 3644;
(e) R.Q. Zou, H. Sakurai, Q. Xu, Angew. Chem., Int. Ed. 45 (2006) 2542;
(f) P. Li, H.M. Liu, X.G. Lei, X.Y. Huang, D.H. Olson, N.J. Turro, J. Li, Angew. Chem., Int. Ed. 42 (2003) 542;
(g) J.S. Seo, D. Whang, H. Lee, S.I. Jun, J. Oh, Y. Jeon, K. Kim, Nature 404 (2000) 982.
[6] W.R. Roderick, C.W. Nordeen, A.M. Von Esch, R.N. Appell, J. Med. Chem. 15 (1972) 655.
[7] (a) K.S. Yeung, N.A. Meanwell, Z. Qiu, D. Hernandez, S. Zhang, F. McPhee, S. Weinheimer, J.M. Clark, J.W. Janc, Bioorg. Med. Chem. Lett. 11 (2001) 2355;
(b) S.G. Liu, J.L. Zuo, Y.Z. Li, X.Z. You, J. Mol. Struct. 705 (2004) 153;
(c) V. Gayathri, E.G. Leelamani, N.M.N. Gowda, G.K.N. Reddy, Polyhedron 18 (1999) 2351;
(d) L. Tong, Chem. Rev. 102 (2002) 4609;
(e) F.G. Lootiens, P. Regenfuss, A. Zechel, L. Dumortier, R.M. Clegg, Biochemistry 29 (1990) 9029.
[8] (a) J.D. Geratz, R.R. Tidwell, R.J. Lombardy, J.H. Schwab, S.K. Anderle, K.B. Pryzwansly, Am. J. Pathol. 139 (1991) 921;
(b) M.J. Tebbe, W.A. Spitzer, F. Victor, J. Med. Chem. 40 (1997) 3937.
[9] M. Du, C.P. Li, X.J. Zhao, Q. Yu, CrystEngCommun 9 (2007) 1011.
[10] (a) R. Fu, S. Xiang, S. Hu, L. Wang, Y. Li, X. Huang, X. Wu, Chem. Commun. (2005) 5292;
(b) M. Munakata, L.P. Wu, G.L. Ning, T. Kuroda-Sowa, M. Maekawa, Y. Suenaga, N. Maeno, J. Am. Chem. Soc. 121 (1999) 4968;
(c) M. Munakata, L.P. Wu, T. Kuroda-Sowa, M. Maekawa, Y. Suenaga, K. Sugimoto, Inorg. Chem. 36 (1997) 4903.
[11] A.W. Addison, P.J. Burke, J. Heterocycl. Chem. 18 (1981) 803.
[12] (a) G.M. Sheldrick, SHELXS 97, Program for Crystal Structure Solution, University of Göttingen, Germany, 1997;

(b) G.M. Sheldrick, SHELXL 97, Program for Crystal Structure Refinement, University of Göttingen, Germany, 1997.
[13] A.J. Fontana, L.D. Hansen, R.W. Breidenbach, R.S. Criddle, Thermochim. Acta 172 (1990) 105.
[14] (a) C.L. Xie, H.K. Tang, Z.H. Song, S.S. Qu, Thermochim. Acta 123 (1988) 33;
(b) H.K. Tang, C.L. Xie, Z.H. Song, S.S. Qu, Y.T. Liao, H.S. Liu, Acta Phys. Chim. Sin. 3 (1987) 113.
[15] (a) U. Mukhopadhyay, I. Bernal, Cryst. Growth Des. 5 (2005) 1687;
(b) R.J. Doedens, E. Yphannes, M.I. Khan, Chem. Commun. (2002) 62;
(c) B.H. Ye, B.B. Ding, Y.Q. Weng, X.M. Chen, Inorg. Chem. 43 (2004) 6866.
[16] (a) R.J. Speedy, J.D. Madura, W.L. Jorgensen, J. Phys. Chem. 91 (1987) 909;
(b) A.H. Narten, W.E. Thiessen, L. Blum, Science 217 (1982) 1033.
[17] D. Eisenberg, W. Kauzmann, The Structure and Properties of Water, Oxford University Press, Oxford, 1969.
[18] L.F. Ma, Y.Y. Wang, L.Y. Wang, J.Q. Liu, Y.P. Wu, J.G. Wang, Q.Z. Shi, S.M. Peng, Eur. J. Inorg. Chem. (2008) 693.
[19] (a) G.A. Jeffrey, An Introduction to Hydrogen Bonding 1, Oxford University Press, Oxford, 1997;
(b) Y.G. Huang, Y.Q. Gong, F.L. Jiang, D.Q. Yuan, M.Y. Wu, Q. Gao, W. Wei, M.C. Hong, Cryst. Growth Des. 7 (2007) 1385.
[20] (a) H. Wang, J.Q. Liu, Y.N. Zhang, Y.Y. Wang, G.L. Wen, C.Y. Guo, Q.Z. Shi, Inorg. Chem. Commun. 11 (2008) 129;
(b) I. Ravikumar, P.S. Lakshminarayanan, E. Suresh, P. Ghosh, Cryst. Growth Des. 6 (2006) 2630;
(c) S. Neogi, G. Savitha, P.K. Bharadwaj, Inorg. Chem. 43 (2004) 3771;
(d) Pallepohu Raghavaiah, Sabbani Supriya, Samar K. Das, Chem. Commum. (2006) 2762.
[21] B. Liu, X.C. Zhang, Y.H. Chen, Inorg. Chem. Commun. 10 (2007) 498.
[22] (a) A.H. Narten, W.E. Thiessen, L. Blum, Science 217 (1982) 1033;
(b) L.F. Ma, L.Y. Wang, X.K. Huo, Y.Y. Wang, Y.T. Fan, J.G. Wang, S.H. Chen, Cryst. Growth Des. 8 (2008) 620.
[23] H.L. Zhang, X.F. Yu, X.X. Li, X.R. Pan, Thermochim. Acta 416 (2004) 71.